powders

MDPI

Article

Flow Behavior of Co-Processed Excipients Using Lactose and Microcrystalline Cellulose as Bulk Fillers

Paulo J. Salústio [1,*], Daniel Cingel [2], Telmo Nunes [3], José Catita [4,5], José P. Sousa e Silva [2,6] and Paulo J. Costa [2,6,*]

1 Research Institute for Medicines (iMed.UL), Faculty of Pharmacy, Universidade de Lisboa, Av. Prof. Gama Pinto, 1649-003 Lisboa, Portugal
2 UCIBIO—Applied Molecular Biosciences Unit, MedTech-Laboratory of Pharmaceutical Technology, Faculty of Pharmacy, University of Porto, Rua de Jorge Viterbo Ferreira, 228, 4050-313 Porto, Portugal; cinged@faf.cuni.cz (D.C.); paulo.silva@ff.up.pt (J.P.S.e.S.)
3 Faculty of Sciences, Universidade de Lisboa, Campo Grande, 1749-016 Lisboa, Portugal; mevarrimento@fc.ul.pt
4 Paralab, SA, 4420-437 Gondomar, Portugal; jcatita@ufp.edu.pt
5 FP-BHS—Biomedical and Health Sciences Research Unit, FFP-I3ID—Instituto de Investigação, Inovação e Desenvolvimento, Faculdade Ciências da Saúde, Universidade Fernando Pessoa, Rua Carlos da Maia 296, 4200–150 Porto, Portugal
6 Associate Laboratory i4HB—Institute for Health and Bioeconomy, Faculty of Pharmacy, University of Porto, 4050-313 Porto, Portugal
* Correspondence: pjsalustio@ff.ulisboa.pt (P.J.S.); pccosta@ff.up.pt (P.J.C.)

Abstract

Powder flow is a constant concern in the production of solid dosage forms. Its concise and reliable determination and improvement are challenges for the pharmaceutical industry. Lactose (Lac) and microcrystalline cellulose (MCC) are both widely used pharmaceutical fillers either alone or mixed. In this study, flow determination was performed through methods described on the European Pharmacopoeia. The results obtained showed poor flow and cohesive behavior for Lac and MCC powders and their mixtures (co-processed excipients). The 50% Lac_MCC mixture, with colloidal silicon dioxide (CSD) as the glidant in different proportions, showed relevant improvements in flow. In addition, the effective angle of wall friction (φx), the effective angle of internal friction (φe), arching, and ratholing were also determined, demonstrating the flow behavior in the discharge equipment. Outlet diameters that prevent blockages or insufficient powder flow were also determined. With this study, it was concluded that it was possible to prepare a co-processed excipient with optimal flow behavior composed of Lac_MCC and CSD as a glidant.

Keywords: co-processed excipients; glidants; flow behavior; shear cell; index flow

Check for updates

Academic Editor: Massimo Poletto

Received: 31 October 2025
Revised: 13 January 2026
Accepted: 16 January 2026
Published: 22 January 2026

Copyright: © 2026 by the authors. Licensee MDPI, Basel, Switzerland. This article is an open access article distributed under the terms and conditions of the Creative Commons Attribution (CC BY) license.

1. Introduction

For many diseases, solid oral dosage forms (SODFs) are the best option for their treatment due to their features, such as dosage accuracy, compliance, stability, and price, among others [1]. Their formulation and manufacture, involving active pharmaceutical ingredients (APIs) and excipients, to produce a medicine with quality, safety, and efficacy, pose many challenges, both in the choice and characterization of raw materials, as well as in certain critical manufacturing steps. Many of these challenges, such as formulation development, good flow, correct particle aggregation, and desired disaggregation of granules and tablets, can be solved by using the right excipients [2,3]. But what is the right

excipient? The right excipient is one with the appropriate physicochemical and mechanical characteristics to create SODFs with suitable structural and functional characteristics that facilitate dissolution and permeation (improving bioavailability). An excipient can be a colorant, diluent, binder and adhesive, lubricant, glidant, and disintegrant [4–8].

As a rule, all excipients should be inert, but some have a recognized action or effect in certain circumstances that is undesirable [9]. Since most of them are present in greater amounts than the API, and therefore influence its release, their choice must be judicious in terms of their physicochemical properties and rheology (flow). The aim of this selective choice is to ensure a good manufacturing process, adequate API release and stability, and patient compliance, as well as other aspects that guarantee quality, safety, and efficacy during use or storage [3,4]. In addition to these pharmaceutical factors, this choice also depends on cost, accessibility and purpose, regulatory approval, and suppliers.

Excipients are generally classified according to their functions. One of the categorizations involves delineating these primary substances into those that affect compressibility (such as diluents, lubricants, glidants, binders, anti-adherents) and those that impact biopharmaceutical, chemical, and physical stability (such as disintegrants, flavorings, sweeteners, colorants) [10]. They also can be classified into modified, co-processed, and novel excipients [11]. In addition, the terms "multifunctional excipients" and "high-functionality excipients" are also often referenced in the literature [12]. Besides these classifications these raw materials are also classified into four categories, as described below [6]: (a) Single chemical entity, that corresponds to excipients with a single excipient [6]; (b) Physical mixture of excipients corresponding to the mixture of two or more excipients without any considerable alteration, i.e., each one remains physically different and separate at a particulate level [13]; (c) New chemical entities or novel excipients, corresponding to a new excipient used for the first time or via a novel mode of administration [14]; (d) Co-processed excipients, that correspond to two or more known excipients which, through co-processing methods (granulation, spray drying, melt extrusion, and milling), undergo modifications to their physical properties without altering their stability or chemical composition; this procedure was initially created to improve the flow, compressibility, and disintegration of solid formulations [15].

Formulations containing one or more of these excipients intended to produce SODFs can have inappropriate pharmacotechnical properties, such as poor flow. When this happens, the processing of these dosage forms is compromised, affecting the content uniformity, the granulation and tableting performance, as well as the hardness, friability, API release of the tablets and granules, and the mass of capsules and tablets [16]. This parameter depends on the particle's characteristics, such as size, surface texture, shape and density, interactions with each other, and interactions with surfaces of the equipment, such as the design of the hopper, the angle of the wall, and the diameter of the orifice. In addition, environmental conditions such as relative moisture and temperature as well as other factors such as static electricity and the force of gravity can also influence flowability [17–19]. This is a mandatory property because it conditions the processing of SODFs, that should be evaluated and improved if necessary.

Among the various techniques employed to enhance flow characteristics, the incorporation of glidants is frequently regarded as a primary option. Colloidal silicon dioxide (CSD), magnesium stearate (MgSt), and talc are the most used glidants [20]. The concentrations of these adjuvants in the mixtures are minimal (0.1–0.5% for CSD, 0.25–5% stearate, and 1–10% for talc), and their distribution must be uniform to produce the best lubricating effect [21–24]. The action of glidants to produce their effects can be expressed by different mechanisms: reduction in cohesion forces (van der Waals attractions) between particles, reduction in surface roughness by filling in the irregularities and depressions on the surface

of the particles, reduction in void spaces between them, and consequently, reduction in interparticle friction coefficient [20,25–27]. Of the products cited above, CSD has good glidant characteristics due to its amorphous nature, the small size of its particles, and the sphericity of the same [20,21,28]. Their nano scale (approx. 10–40 nm) [29,30], which can have a negative effect due to particle aggregation, is extremely relevant to their action as lubricants. For values less than 10 nm, glidants reduce contact force because they fail to separate particles through their spacer action, thus having the opposite effect [31]. During the mixing process, these aggregates break down and their particles disperse, adhering to the surfaces of the filler (diluent) or API particles, which are typically micron-sized. With specific surface area values (BET, $m^2\ g^{-1}$) ranging from 90 to 330 and a tamped density of approximately 50 to 280 g cm^{-1} (Evonik), these glidants have excellent characteristics for improving the flow of powders and powder mixtures. Its action, based on the mechanisms already described, results from a separation of the surface of the filler (diluent) particles by the creation of glidant points (roughness, asperities) through van der Waals forces, with a concomitant reduction in the cohesive/adhesive forces between the filler particles [32,33]. However, an optimal amount of glidant depends on the mixing conditions and the morphology of the powders [34]. In more recent developments, nanomaterials (NMs) have emerged as significant components within glidants across numerous industrial domains, including pharmaceuticals and cosmetics, among others [25,35]. The European Commission described NMs as natural, incidental, or manufactured material containing free particles, in aggregate or agglomerate form, of which at least 50% of the particles, in numerical size distribution, have one or more external dimensions between 1 and 100 nm [36].

Among the various methods to assess the flow characteristics of the bulk powders, powder mixtures, mixtures with glidants, and granulates without or with glidants prior to their processing are those described in the Ph Eur. The most frequently used are the repose angle, compressibility index (CI) and Hausner ratio (HR), flow through orifice, and shear cell [18,37–40].

Conventional methods produce results influenced by several factors that can lead to values that are not representative of the parameter under analysis. For example, the angle of repose is a quick and easy method that does not represent an intrinsic property of the powder. It is based on determining the angle formed in relation to the horizontal base by a cone-like pile of powder, created when it passes through a funnel-like container [41]. The formation of this cone depends on particle segregation, consolidation, powder aeration, and gravitational force. Therefore, the values determined depend on the bulk powder density, the friction and cohesive forces between particles, and the friction forces between particles and funnel walls, as well as the cohesive strength of the powder itself. When the angle is greater than 40°, the powder flow is classified as poor (cohesive powder) [42,43]. Regarding the aerated and tapped densities of the powders that allow the calculation of the CI and HR, their values can vary greatly due to the number of voids existing between their constituent particles and the non-uniformity of the taps. The parameters are related to the consolidation state of the material with and without tapping. Aerated density results from dividing the mass by the volume it occupies without tapping, while the tapped density results from dividing the mass by the volume it occupies after tapping [42,44]. Both CI and HR allow an understanding of powder flow behavior in terms of its cohesiveness, that is, in terms of particle–particle friction that occurs in a moving powder mass and not in a static condition. These parameters depend on several factors, such as apparent densities of the powder, variation in powder volume due to gravity under tapping, and lack of control of external stress during tapping [42,45]. The HR, which is derived from the ratio of tapped density to aerated density, serves as a valuable metric for comprehending particle friction by quantifying the resistance that the particles exert on their movement. HR

values above 1.46 mean that the powder has a very poor flow, and below 1.25, that it has a fair flow [42,46]. CI, like the previous one, demonstrates the resistance that the powder particles, due to their interactions, imposes on the flow. It is an indirect determination of the flow and compressibility resulting from the reduction in the powder volume obtained by the difference between the aerated and tapped densities. CI values below 20% correspond to fair powder flowability [45].

Of the various methods mentioned, the measurement using a shear cell tester produces the most reliable results, with an accurate and precise assessment of powder flow. This method is based in the determination of the flow index (ff_c) that relates the unconfined yield strength (σ_c) with the major principal consolidation stress (σ_1). Its numerical values allow for determining the powder flow based on a scale of 0 to >10 [18]. Unconfined yield strength (σ_c) or compressive strength represents the stress that promotes failure, named "incipient flow", of the consolidated bulk solid. When this occurs, the consolidated bulk solid begins to flow. The flow function (FF), which is solely determined by cohesion and pre-consolidation stresses [47,48], devoid of any friction coefficients, is derived from the σ_c versus σ_1 curves, utilizing the MohrCoulomb approach. For a storage duration (t) of 0, this is referred to as the instantaneous flow function (IFF), while for a storage duration (t) exceeding 0, it is termed the time flow function (TFF) [17,21,22,49–51]. Through the shear cell method, it is also possible to determine other parameters that help in flow characterization such as the effective angle of internal friction (φe), effective angle of wall friction (φx), critical arching and critical ratholing, HR, and CI. Within these parameters, φe and φx allow for predicting the slopes of the equipment wall surfaces and the outlet dimensions [52,53] for an efficient flow. The discharge process is more influenced by external stress (σ_0), which depends on the powder density and the outlet diameter, than by σ_1. For Jenike, formation of the arch only occurs when ff_c is less than 1.3 (very cohesive powder) [19,54]. Thus, the larger the σ_1, the larger σ_c will be, and, therefore, the greater the probability that σ_c will exceed σ_0. When this occurs, there is a greater ease of obstruction in the powder flow under the influence of two contradicting factors (σ_0 and σ_c) [18,55]. σ_1 versus σ_0 represents the factor flow and σ_0 the stress "at the abutment of the dome" according to Jenike [56,57].

Since powder flow is a real problem in processing and production of SODFs, improving this parameter brings benefits to the pharmaceutical industry in terms of product quality and production costs. Therefore, the aim of this work was to prepare and evaluate the flow behavior of a mixture of two excipients both with poor flow, lactose (Lac) and microcrystalline cellulose (MCC), in different proportions, to verify whether there was a synergistic effect on the improvement of the flow. Lac and MCC are both widely used pharmaceutical fillers, with their effectiveness determined by their specific formulation and properties due to their distinct flow behaviors and compressibility characteristics. Lac exhibits brittleness, whereas MCC functions as a plastic deformer with superior compressibility, and their interplay or specific grades can notably influence flow characteristics [58,59]. In a second phase and due to the obtained results, the addition of colloidal silicon dioxide (CSD) as a glidant in different ratios was studied to improve the flow behavior of the mixture, Lac_MCC (50:50%, w/w).

2. Materials and Methods

2.1. Materials

Lactose (batch: 217155-P-1) and microcrystalline cellulose (batch: 181117-P-2) were purchased from Acofarma, Barcelona, Spain. Colloidal silicon dioxide (CSD), Aerosil R972 Pharma) (batch: 1032083012) was a gift from Evonik, Essen, Germany.

2.2. Methods

2.2.1.Powders and Mixture Preparation

Lac and MCC powders were characterized by sieving, scanning electron microscopy (SEM), and laser diffraction and CSD by SEM and laser diffraction. These powders were used to prepare the powder mixtures in two steps: the first involved the preparation of five fractions corresponding to bulk Lac and MCC powders and Lac75_MCC25, Lac50_MCC50, and Lac25_MCC75 powder mixtures; after weighing of the components of the last three fractions (w/w), the same were mixed for 15 min in a TURBULA® mixer (WAB, Muttenz, Switzerland); the second step involved the preparation of the other four fractions using Lac50_MCC50 powder mixture and CSD in ratios of 0.25, 0.5, 0.75, and 1% (w/w); after weighing of the components, each fraction was mixed for 5 min in a TURBULA® mixer.

The choice of Lac50_MCC50 for the addition of CSD was because it was the mixture that presented the best flow results, which translated into a higher ff_c.

Particle Size Characterization

1. Analysis by Sieving

The bulk powders (Lac and MCC) were analyzed by sieving according to Ph. Eur. 11 (710, 500, 355, 250, 180, 125, 90, and 63 µm, sieves Retsch). A sieve shaker (Retsch AS 200 digit, Haan, Germany) in a vibratory amplitude of 2 mm was used [60].

2. Analysis by Scanning Electron Microscopy

The bulk powders (Lac, MCC, and CSD) after drying were analyzed by SEM (Phenom XL G2 desktop SEM, Thermo Fisher Scientific, Waltham, MA, USA) to evaluate the morphology of their particles. This equipment, equipped with a secondary electron detector, allowed the analysis of the powder particles of the various samples separately, at various magnifications, after they had been coated with gold by a sputtering coating chamber, model JOEL-JFC-1200 Fine Coater, Peabody, MA, USA.

3. Analysis by Laser Diffraction

The particle size distributions (PSDs) of the bulk powders (Lac and MCC) and powder mixtures (Lac_MCC) in different proportions [61] were analyzed by laser diffraction (LD) using Mastersizer 3000 (Malvern Instruments, Worcestershire, UK) with a coupled dry powder dispersion system (Malvern Aero S). For CSD, in addition to the sample dispersion units referenced, the Malvern Hydro EV (wet sample dispersion) was also used. The amount of each sample (10–20 mg) was introduced into the aero S accessory at a dispersive compressed air pressure of 0.2 bar, with obscuration values ranging from 0.5% to 7%, and a vibration feed rate set at 25%. The material was classified as non-spherical, utilizing a refractive index of 1.430 and an absorption index of 0.001, according to the Mie Scattering Model. The aim was to attain the minimal conceivable residual and weight residual values, concurrently conducting a computation of the volume-weighted particle distribution parameters, including the percentiles 10, 50, and 90 of the equivalent spherical diameter derived from the volume (Dv10, Dv50, Dv90) and span (a metric indicative of the breadth of size distribution):

$$\text{Span} = (\text{Dv90} - \text{Dv10})/\text{Dv50} \quad (1)$$

Moisture

The losses of weight of the bulk powders and powder mixtures (amount = 3–5 g) were determined in a heating cycle of up to 80°C until a constant weight, using a moisture analyzer (AD-4713, Tokyo, Japan).

Powder Flow Characterization

1. Angle of Repose

Each bulk powder and the powder mixtures were passed onto the plate through a funnel with a 15 mm diameter nozzle (Erweka GT granule tester, Hessen, Germany) [38]. This parameter was classified according to 2.9.36. Powder flow of Ph. Eur. [40] using the following equation:

$$\text{tg}(\alpha) = (\text{height})/(0.5 \times \text{base}) \quad (2)$$

2. Bulk and Tapped Density

This parameter was determined according to 2.9.34 Bulk density and tapped density of powders of Ph. Eur. [39] using a graduated cylinder (250 cm^3) filled with each of the bulk powders and powder mixtures without glidant, up to 150 cm^3 of its capacity, after weighing the mass and calculating the respective bulk and tapped densities (TAP Density Tester, Model:ETD:1020, Electrolab, Mumbai, India). The CI was calculated using the equation below (ρ-density):

$$\text{Compressibility Index (\%)} = 100 \times (\rho_{\text{tapped}} - \rho_{\text{bulk}})/\rho_{\text{tapped}} \quad (3)$$

This parameter was also determined for bulk powders and powder mixtures without glidant by the bulk powder density (BD) method using the shear cell and classified according to 2.9.36. Powder flow of Ph. Eur. [40].

3. Flow Properties

The flow properties according to this test were examined on the bulk powder (Lac and MCC), powder mixtures (Lac_MCC) in different proportions, and Lac50_MCC50 with glidant in different ratios. The processing of this method using a Brookfield Powder Flow Tester (Middleboro, MA, USA), connected to Powder Flow Pro Software (V1.3 Build 23), consists of compressing the bulk powder and powder mixtures with and without glidant, with a defined volume and weight contained in an annular shear cell, through a lid that moves vertically in a downward direction. Then, when the lid touches the powder, the cell rotates at a certain speed and the torque is measured, thus allowing the flow properties to be assessed: Standard Flow Function (FF) method, Quick Time Consolidated Flow Function (QC) method (12 h hold, $n = 1$), and Quick Wall Friction (WF) method (this last only used on the bulk Lac and MCC and Lac_MCC in different proportions). The σ_c and effective angle of internal friction (φe) were also determined as a function of σ_1 while the effective angle of wall friction (φx) was determined as a function of normal stress (σ_w) allowing other flow behaviors to be evaluated [19]. The flowability index (ff_c) of each run was determined using the equation described below (σ_1—major principal consolidation stress; σ_c—unconfined yield strength), and the flow behaviors of each bulk powder and powder mixtures with and without glidant were classified as follows [18]: not flowing ($ff_c < 1$); very cohesive ($1 < ff_c < 2$); cohesive ($2 < ff_c < 4$); easy-flowing ($4 < ff_c < 10$); free-flowing ($10 < ff_c$).

$$ff_c = \sigma_1/\sigma_c \quad (4)$$

With the exception of the QC method, as previously mentioned ($n = 1$), all bulk powders and powder mixtures with and without glidant were analyzed in triplicate ($n = 3$). Results are shown as the mean ± standard deviation (sd).

3. Results and Discussion

3.1. Powders and Powder Mixture

3.1.1. Particle Size Characterization

Analysis by Sieving

Lac and MCC bulk powders showed different sieve shaking times of 20 and 10 min, respectively, which was necessary to meet the Ph. Eur. criteria [60]. For each excipient, the weights retained in different sieves are shown in Figure 1. The results showed that Lac had the highest retention between sieves F > 180 and F > 250 (35.1%), reaching more than 2/3 of the bulk sample amount between sieves F > 90 and F > 250. Between F > 63 and F < 90, 9.4% was retained, and the remaining sieves added up to a value of 5.9, which was higher than the 1.8 between F > 250 and F > 355. On the other hand, the MCC presented a higher amount below F < 63 (66.5%), reaching more than 2/3 of the bulk sample below F > 90. Between F > 90 and F < 125, 8.5% was retained, and the remaining sieves added up to a value of 6.6%, with the highest being 4.2 between F > 125 and F > 180.

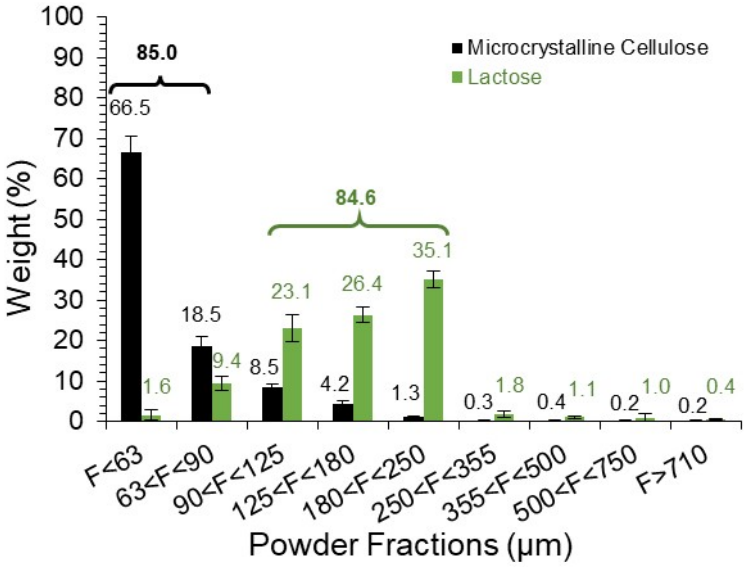


Figure 1. Fractional distribution (%) for lactose (green) and microcrystalline cellulose (black).

With these results, it was possible to observe that these two excipients had a very different particle size distribution (PSD), with the MCC containing mainly particles smaller than F > 90 and Lac containing particles between F > 90 and F > 250. Understandably, these particle size intervals will be decisive for the flow behavior of these two excipients and the resulting mixtures.

Analysis by Scanning Electron Microscopy

The SEM powder images for bulk powders (Lac and MCC) and glidant (CSD) can be observed in Figure 2.

MCC is predominantly composed of acicular particles with rounded corners and virtually smooth surfaces, without significant roughness. There are a much smaller number of other particles with different advanced shapes, but they are practically identical to the others. No small particles adhere to the surfaces of larger particles, and there are no aggregates, but some of them appear to be intertwined, creating non-genuine porosities. This intertwining around their own axis results in the plastic behavior of this material.

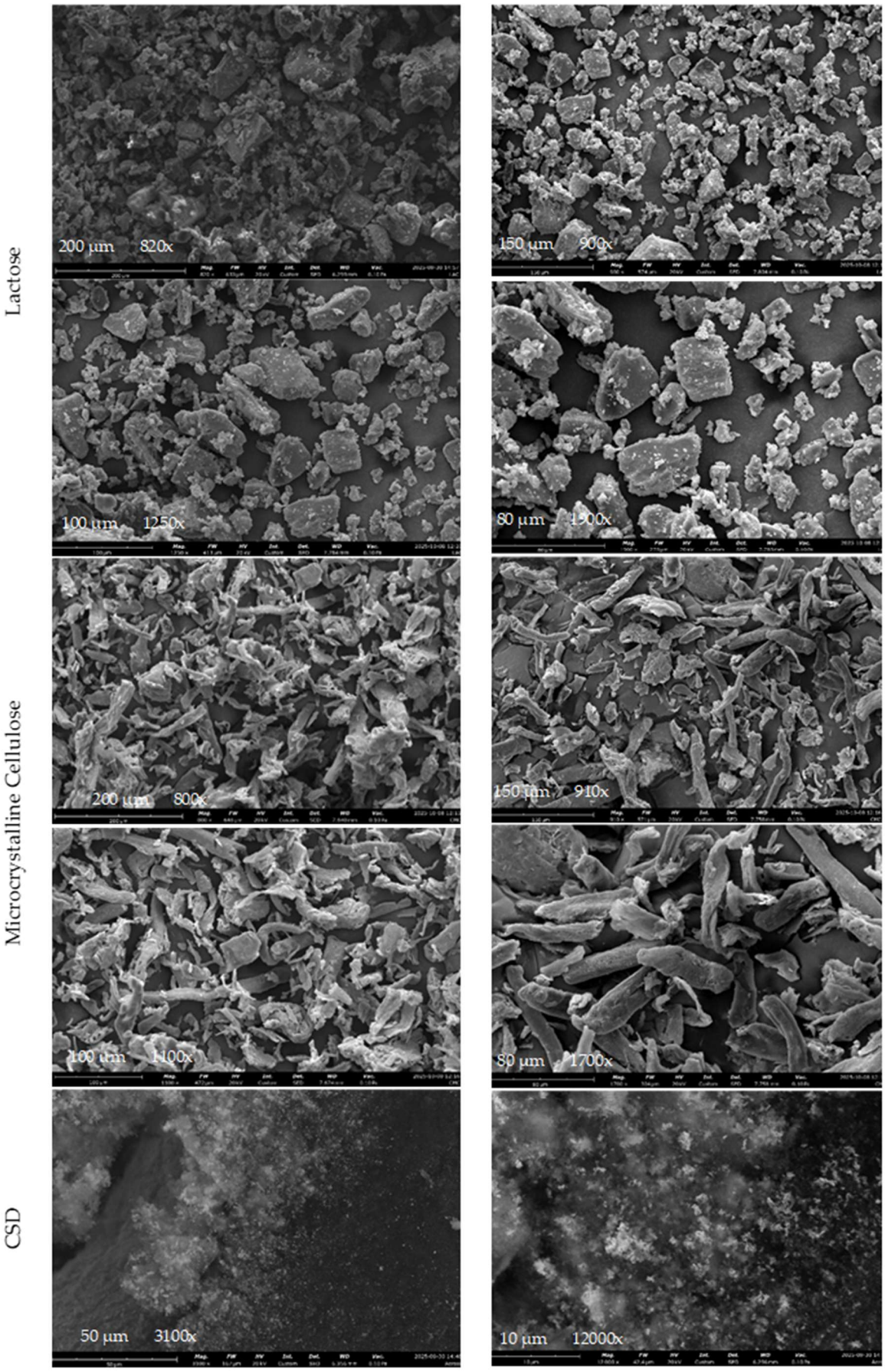


Figure 2. Scanning electron micrographs of the bulk powders (Lac and MCC) and glidant (CSD).

Lac is composed predominantly of particles with different shapes, mainly equant and plate, but also contains other irregular shapes of very varied sizes, with many small particles. Its surfaces are smooth and show sharp edges. Those without porosity and the particles with the smallest size tend to form aggregates or adhere to the surface of the largest particles. This material has brittle behavior.

Both powders present particles with little spherical tendency, and the characteristics of the masses were decisive in the flow behavior of these excipients and have already been analyzed in other studies by the same authors, corroborating these descriptions: F < 63 of MCC200 [17]; F > 90 of LacMN200 [51].

Regarding CSD, its particles were very small and difficult to define, resembling more like a cloud of powder. Their shapes are likely variable, with a spherical tendency. Smaller particles adhere to larger particles, forming aggregates and making their surface slightly rough, thus reducing the possibility of interparticle interactions [20]. The spherical shape and surfaces of its particles explain its good glidant action. This material was also analyzed in other studies conducted [21,22].

Analysis by Laser Diffraction

The PSDs of the bulk powders (Lac and MCC) and powder mixtures (Lac_MCC) in different proportions without glidant are shown in Figure 3.

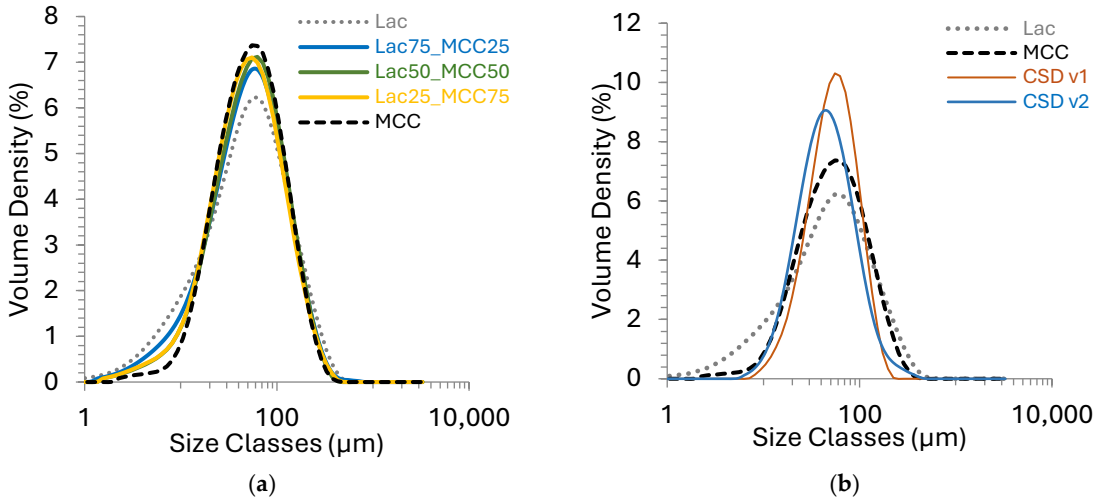


Figure 3. Particle size distributions for (**a**) bulk powders (Lac and MCC) and their mixtures (Lac_MCC) in different proportions; (**b**) CSD using different sample dispersion units (CSD v1v Aero S; CSD v2—Hydro EV).

Of the various samples, the one with the narrowest size distribution is MCC, which also had the largest average size. This excipient has the smallest particle size. These results compared with those obtained by the sieving method show that its particles, likely due to their small size (<63 µm = 85%, Figure 1), aggregated during the test, as the distribution is almost identical to that of Lac (>90 and <180 µm = 84.6%, Figure 1). Lac had the widest distribution size and the smallest average size. All Lac_MCC mixtures overlapped, presenting the same size distribution and practically the same average size, located between Lac and MCC. The highest volume density (%) was observed for MCC. In this test, the PSD of each mixture related to each of the bulk excipients showed similarity, with practically overlapping profiles (Table 1 and Figure 3a). The higher percentage of isolated excipients with different particle sizes was not reflected in the final mixture analysis, likely due to the aggregation of the smaller particles, as previously mentioned [61].

Table 1. Size percentiles 10, 50, 90, and Span of the bulk powders (Lac and MCC) and their mixtures (Lac_MCC).

	Lac	Lac75_MCC25	Lac50_MCC50	Lac25_MCC75	MCC
Dv10 µm	9.9	12.9	15.3	15.1	18.2
Dv50 µm	40.5	50.6	52.6	49.6	52.5
Dv90 µm	158.0	145.0	144.0	140.0	140.0
Span	2.996	2.615	2.441	2.513	2.328

When comparing the sample dispersion units used with CDS PSD, the results were close, with Hydro EV (wet sample dispersion) giving lower results (Figure 3b), but very different to the ones obtained by SEM. Regarding the wet sample dispersion of CSD, the results were in the order of 18.9 µm for Dv10, 44.4 µm for Dv50, 105 µm for Dv90, and 1.926 for Span, and this was likely due to the aggregation of the smaller CSD particles. Laser diffraction measures the larger, effective size of an aggregate in solution, while SEM captures the dry, hard structure of the same aggregate.

3.1.2. Moisture

The bulk powders (Lac and MCC) and powder mixtures (Lac_MCC) showed the following moisture contents (%): Lac = 0.18 ± 0.00; MCC = 5.33 ± 0.55; and Lac75_MCC25 = 1.54 ± 0.17; Lac50_MCC50 = 2.98 ± 0.18; Lac25_MCC75 = 4.56 ± 0.17. The bulk powder with the highest moisture content was MCC (5.33 ± 0.45%), and the mixture was Lac25_MCC75 (4.56 ± 0.14%), which contained this excipient in a greater amount. A similar result for these excipients was obtained in previous studies by the same authors (Lac: F > 90 = 0.27 ± 0.13%; MCC: F > 63 = 5.6 ± 0.20; and F < 63 = 5.4 ± 0.13) [17,51]. The moisture values for both excipients and the mixtures were not considered in the flow assessment, as they were low and did not have a great influence on this parameter. According to Amidon and Houghton [62], levels below 5% have little effect on the mechanical and flow properties of the MCC (Avicel PH101). Subsequent results [63–65] showed that the flow properties of Lac and MCC deteriorated with consecutive increases in relative humidity (RH) due to increased interparticle interactions.

3.1.3. Powder Flow Characterization

Angle of Repose

The results obtained in this parameter for the bulk powders (Lac and MCC) and powder mixtures (Lac_MCC) with and without glidant are presented in Table 2. These results are located between poor (must agitate, vibrate) 46–55° and very poor 56–65° [40] and depended on the shape and size of the powder particles involved, bulk powder density, action of gravity inherent in the method, walls, equipment, and environment conditions [40,66,67].

When comparing these results with previous studies of same authors [17,51], it can be found that they are within the same magnitudes. The reason for these values is that the flow behavior of powders (in bulk or in mixtures) is influenced by their density, friction and adhesive/cohesive forces between their particles, friction forces between the particles and funnel surfaces, and strength of the powder itself. All these forces result from interactions between the surfaces of their particles and, therefore, depend on their size and shape [19]. As Lac and MCC particles showed little spherical trend (Figure 2), the results for this parameter fall within the classification of poor to very poor [40]. The reasons for this classification are related, as already described, to the size and shape of the particles of each of the excipients. Due to their smaller size (Figure 1), and therefore greater surface area, MCC particles develop more surface friction between themselves and between themselves

and the equipment surface, worsening the flow. The low flow of this excipient, resulting from the size of its particles, is also influenced by their shape (Figure 2), which, in this case, is not spherical (low flow). Furthermore, their surfaces are smooth, increasing the contact area and thus increasing frictional forces, which imply a decrease in flow. For MCC, the shape and size factors are synergistic. Regarding lactose, poor flow is more influenced by the shape factor than the size factor. Increasing the particle size usually improves flow due to a decrease in specific surface area; therefore, fewer frictional interactions result in better flow. However, the practically non-spherical shape and many small particles adhering to the surfaces of larger particles (asperities, Figure 2) hinder flow by increasing interlocking forces [50]. For this excipient, the shape and size factors act in opposition. The predominance of one factor over the other determines the flow. In a recent study by the same authors [50], and contrary to the literature, it was proven that reducing the particle size improved flow because of the shape factor overlapping the size factor. In turn, the powders resulting from mixing also produced high repose angle values, classifying them on the same scale as previously mentioned. For the MCC and mixtures with high amounts, these poor results are related to their small size (higher surface area), which increases the interparticle interactions, and their shapes (Figure 2). These interactions, as referenced before, are predominantly frictional between particles and between particles and funnel surfaces. Here, cohesive forces are not relevant. According to Lac and mixtures with high amounts of Lac, the reason for poor and very poor flow [40] is due to the irregular shape of its particles with little spherical trend, their agglomeration, and adhesion of smaller particles to the surface of larger particles (Figure 2). The addition of glidant (CSD) in different proportions to Lac50_MCC50 created a big decrease in the repose angle (Table 2), providing a better flow behavior, corresponding to the border between passable (may hang up, 41–45°) and poor (must agitate, vibrate, 46–55° [40]). The improvement in flow caused by CSD resulted mainly from the reduction in frictional forces and interlocking between particles, as well as the reduction in the coefficient of friction between them due to the reduction in the roughness of their surfaces by filling their irregularities and the empty spaces between them [26,27]. For this parameter, the results (Table 2) demonstrated that the best glidant proportion was 0.5%, with no big differences in relation to other percentages.

Table 2. Repose angles of the bulk powders (Lac and MCC) and their mixtures with and without glidant.

Excipients and Mixtures		**CSD**	**Lac50 + MCC50 + CSD**
	mean ± sd		mean ± sd
	(°)	(%)	(°)
Lac	52.3 ± 3.14		
Lac75_MCC25	53.0 ± 1.20		
Lac50_MCC50	56.0 ± 0.26	0.25	46.0 ± 1.64
		0.50	45.2 ± 2.46
		0.75	46.4 ± 1.13
		1.00	47.8 ± 0.44
Lac25_MCC75	53.4 ± 1.39		
MCC	51.6 ± 1.57		

Bulk and Tapped Density

Conv methods are highly dependent on the powder density, changes in powder volume, and the inability to control external stress from the tapping process, and, therefore, do not allow for appropriate comparison between them; CI parameters continue to be

widely used to determine powder flow properties. Although this method does not provide reliable measurements, it is used to compare the results with those obtained using the BD method. However, Hou and Sun (2008) suggest that density has a limited effect on powder flow properties when measured by a ring shear tester [68]. The bulk powders (Lac and MCC) and powder mixtures (Lac_MCC) without glidant presented CI values located in the flowability scale between passable (21–25%) and poor (26–31%) (Figure 4) [39]. The results for Lac and MCC overlapped in both methods, showing that the packing between the Conv method and the BD was similar. However, MCC showed better results due to the characteristics of its particles (Figure 2), which provided better flow, with a CI lower than for the other excipient. Although MCC has a smaller particle size than Lac and therefore a larger surface area and greater interaction forces between its particles, as described in the previous parameter, it exhibits better flow (lower CI) because the shape factor in Lac (irregularities and asperities) cancels out part of the effect produced by the larger size of its particles (Figure 2). This test corroborates the results of the previous parameter, demonstrating the predominance of the shape and size factors of one over the other [50]. The mixtures of these powders (Lac_MCC) showed a decrease in CI as the amount of MCC increased in the mixture. This decrease is understandable, as the cellulose derivative has a better CI for the reason already mentioned. When comparing the values obtained for the two methods, it was observed that the BD method presented lower CIs and, therefore, better compressibility. The reason for these decreases is that there is better movement and packing of the particles under stress (Pa) in the BD method than under the action of tapping in the Conv method [19,68]. The best packing with best densification of the mixture results from more efficient expulsion of air between the particles (voids) and more effective deformation of the same. The difference in particle size between the two excipients (Figure 1) is favorable to this rearrangement, as the smaller particles will fit between the larger particles, making the mixture more compact (dense). However, it should be noted that the two mixtures containing the highest amount of MCC (Lac50_MCC50 = 22.63 ± 1.09% and Lac25_MCC75 = 21.87 ± 0.69%) presented a better IC than MCC itself (23.11 ± 1.07%). The reason for this fact may be attributed to the presence of the two excipients in the mixture in adequate proportions for a more perfect reorganization of their particles due to their shapes and sizes, which are quite different. These differences result in better densification of the mixture (Figures 1 and 2). Of the various mixtures, the one with the best CI was the one with the highest percentage of MCC (21.87 ± 0.69%) for the BD method.

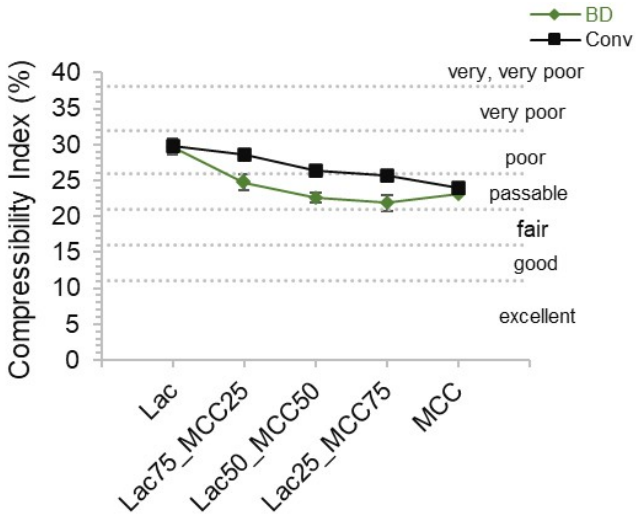


Figure 4. Influence of the excipients (Lac and MCC) in the compressibility index of the powder mixture (Lac_MCC).

Flow Properties

1. Effective Angle of Wall Friction

All interactions (mainly friction and interlocking) between bulk powder (Lac and MCC), powder mixtures (Lac_MCC), and the inner surface of the hopper or other surfaces can be determined by the wall friction angle (φx). This parameter is influenced by stress and decreases as it increases. As can be seen in Figure 5, bulk powders and powder mixtures undergo a marked fall in this parameter to approximately 1200 Pa and, from there, a slight decrease with a tendency to plateau. The decrease in this angle under the action of σ_w results in greater ease of movement of the powder particles (reorganization) due to the elimination of voids, which makes the respective powder denser. This reorganization is accompanied by a simultaneous reduction in the interaction between the particles and between them and the surface of the equipment. For values above 2500 Pa, all profiles practically ceased to depend on σ_w. The powder with the highest value for this parameter was Lac, and the mixture containing the largest amount of this component was Lac75_MCC25, which proved its poor flow characteristics. Regarding MCC and the remaining mixtures (Lac50_MCC50 and Lac25_MCC75), there was an overlap of the profiles, demonstrating the influence of the particles of this excipient on the Lac particles. This overlap of the profiles was accompanied by a decrease in the angle, indicating an improvement in flowability. In determining this parameter, it was observed that two excipients behaved differently under the action of σ_w, with MCC, which has a smaller particle size and a predominantly acicular shape, exhibiting better flowability. Although they are different products (chemistry and texture), the size versus shape provided better flowability for MCC than for Lac (more irregularities on the surface provided interlocking and many small particles adhered to larger particles, worsening the flow).

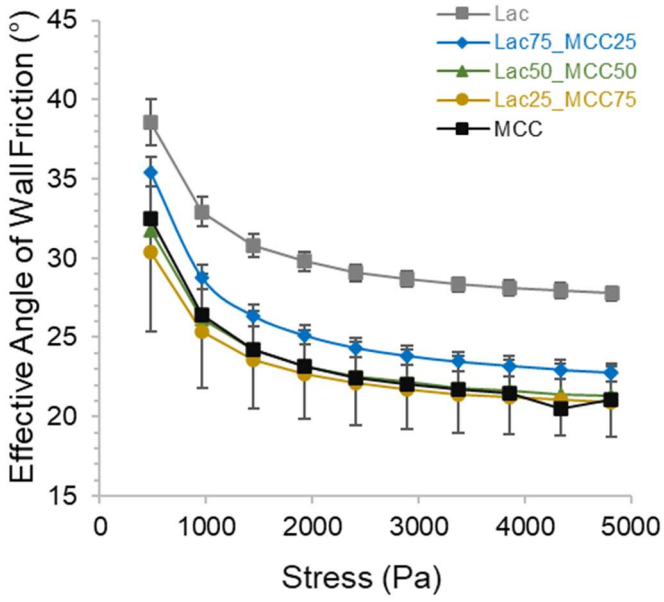


Figure 5. Effective angle of wall friction (φx) vs. normal stress (σ_w) for bulk powders and powder mixtures without glidant.

2. Effective Angle of Internal Friction

In this parameter, as in the previous test, Lac presented the highest values of φe (Figure 6) and, therefore, the worst flow. Of the remaining powders, the mixture with the highest amount of this excipient started differently from the others and MCC, but at 2500 Pa, they overlapped. This angle is influenced by consolidation stress (σ_1) and decreases as it increases. It provides an insight into the problem of consolidation of powders inside

hoppers and silos during handling and processing, which can cause complications for production lines. As can be seen in Figure 6, bulk powders and powder mixtures without glidant experience an initial fall in this parameter. This fall was due to the movement of particles with the elimination of voids. In Lac, it was greater and occurred up to approximately 4800 Pa, and from there on, the absence of a plateau showed that the complete reorganization of its particles was not achieved. This fact results from the shape of its particles (more irregular, and therefore more interactions, Figure 2) influencing more than the size. In relation to the other profiles, they all overlapped. The fall in angle was not marked and occurred up to 2000 Pa, and, from there, after a very slight decrease, it reached a plateau. From this point onwards, φe remained practically constant, showing no dependence on σ_1 as it increased. When this occurs, the powder flow behavior is classified as free flowing [18,69]. The presence of a greater amount of MCC in the mixtures showed a decrease in this angle, providing better flow. Once again, the characteristics (shape versus size) of the MCC particles provided better movement and reorganization of the same, resulting in improved flow.

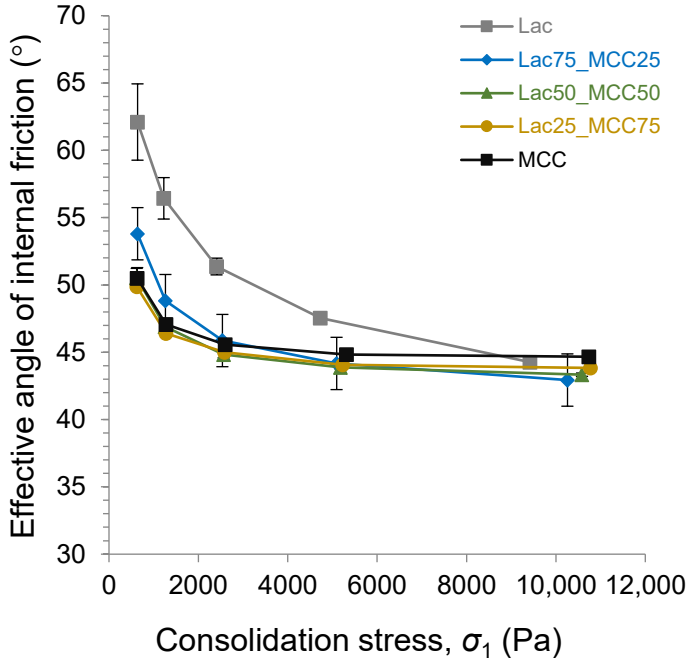


Figure 6. Effective angle of internal friction (φe) vs. consolidation stress (σ_1) for the bulk powders and powder mixtures without glidant.

The Lac50_MCC50 with glidant in different proportions was subjected to this test, producing the results shown in Figure 7. From these results, it was possible to observe a decrease in φe for all powders containing CSD compared to the mixture without glidant. This decrease was not very pronounced up to 1500 Pa of σ_1 and, from there on, it reached a plateau, showing that the powders no longer depend on the consolidation stress (free flowing) [18,69]. The mixture containing 0.25% showed the most pronounced fall at the beginning but overtook the others near 2500 Pa of σ_1. The decrease observed in this angle for all mixtures with glidant resulted from the decrease mainly of friction forces between all their particles (Lac and MCC). This decrease was due to the interposition of CSD between them, filling voids and leading to improved flow. The reduction in these forces allowed better movement of the particles, providing better densification and deformation. Based on the results obtained in this test, it can be stated that the minimum amount of CSD that caused the greatest reduction in angle and therefore better flow was 0.5%.

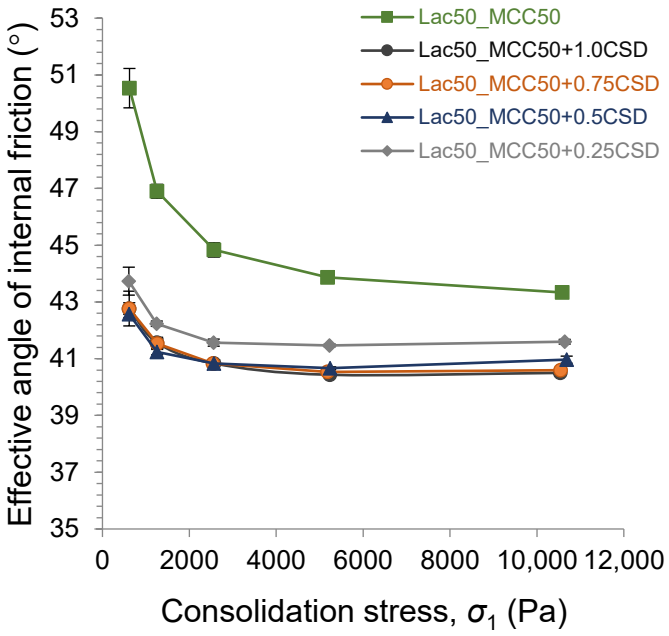


Figure 7. Effective angle of internal friction (φe) vs. consolidation stress (σ_1) for the powder mixture (Lac50_MCC50) with glidant.

3. Arching and Ratholing

Partial or complete obstruction of powder flow may occur when the funnels (hoppers, silos) are opened. The powder flow in this equipment results from the movement of the powder when the outlet is opened. At this point, there should be no arching or ratholing. For this movement to occur without impediment, the walls of the hopper and chutes must be steep and must not offer adhesion/friction. In cohesive bulk powders, arching occurs due to the cohesive strength (compressive strength, unconfined flow strength) of the bulk solid, which depends on the mainly frictional forces that occur between its individual particles. For example, in the case of gravity (stress) acting on the bulk solid, if its action is greater than the resistance of the bulk solid (measured as σ_c), it flows; otherwise, arching occurs. Ratholing occurs when the particles of the powder, due to their size and shape, develop mainly friction forces between their surfaces and the walls of the equipment that exceed the interparticle friction forces, creating different speeds in the powder, which leads to the occurrence during the flow of a channel within the bulk solid [18].

For arching, the results for bulk powders (Lac and MCC) and powder mixtures (Lac50_MCC50) are presented in Figure 8. A decrease in outlet diameter occurs as the concentration of MCC increases (0.328 to 0.186 m), showing a plateau trend between Lac75_MCC25 and MCC. This decreases, reaching the lowest value for Lac50_MCC50 (0.144 ± 0.007 m), which confirms the results obtained in determining φe, where MCC and the mixtures with higher amounts of this excipient showed the best flow (Figure 8). In another study from same authors, when using MCC200, F < 63 showed a value of 0.125 ± 0.008 m that proved a similar arching flow to the MCC value (0.186 ± 0.014 m). The comparison between MCC and the F < 63 of MCC200 is appropriate because 66.5% (w/w) of MCC particles are smaller than 63 µm (F < 63, Figure 1). In addition to the size, the predominantly acicular shape is also common. Given these similarities, the behavior of the two powders in relation to this parameter was similar. The same comparison was also made between Lac and F > 90 (18.84%, w/w) of LacMN200 used in another study by the same authors, whose value for this parameter was 0.050 ± 0.003 m. However, the value for LacMN200 and its FTotal (bulk Lac) had an outlet diameter of 0.180 ± 0.003 m, which also differs significantly from that obtained with the bulk Lac used in this study

(0.328 ± 0.038 m). This can be explained by the fact that it is predominantly composed of particles between F > 90 and F < 250 (84.6%, Figure 1) and that have many smaller particles adhering to their surfaces. The larger particle size and large number of small particles decrease the friction between their surfaces and improve powder densification, improving flow, which leads to a decrease in outlet diameter. The form is not mentioned because its impact has the same effect in both cases. The results obtained for this parameter in relation to Lac and MCC, regardless of their chemical compositions and textures, showed that the shape was more influential than the size [17], demonstrating through the outlet diameter a better flow for the MCC (smaller particle) and for mixtures with a higher amount, as previously cited. The less irregular shape and the smaller or almost non-existent number of small particles that adhere to the surface of larger particles in relation to the MCC (Figure 2) substantially reduce the interaction forces between particles, especially friction and interlocking forces, resulting in better flow. The lowest outlet diameter value verified for Lac50_MCC50 can be explained by enough particles of both excipients with different shapes and sizes occurring simultaneously and which, under stress, undergo a reorganization, resulting in a solid compact with better densification and, therefore, better flow [18]. At this point, the forces of interaction between the particles are reduced to the lowest value compared to bulk powders and other powder mixtures. Despite everything, the differences between the outlet diameters for the various powder mixtures were very small.

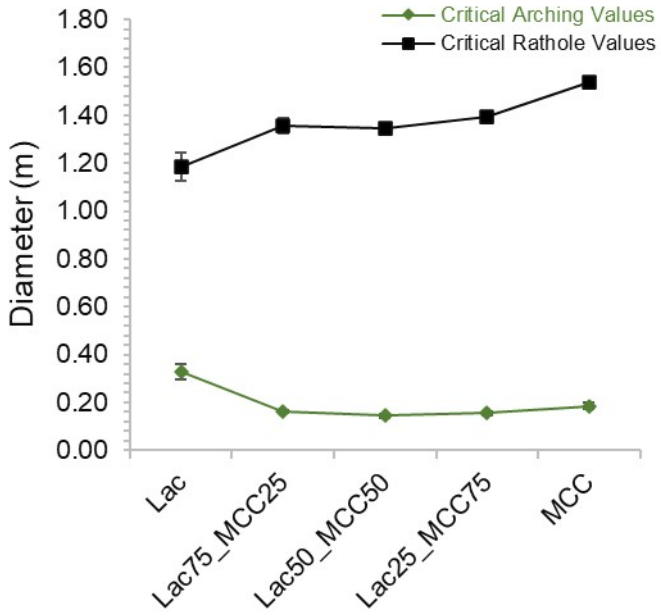


Figure 8. Critical arching and rathole values (in meters) for bulk powder and powder mixtures without glidant discharges.

In ratholing, the flow behavior of the two bulk powders (Lac and MCC) surprisingly reversed position (Figure 8), which is contrary to what was observed in *φe*, where MCC and the mixtures with higher amounts of this excipient showed the best flow (Figure 6). This parameter, unlike the previous case, increased the output as the MCC concentration increased (1.185 to 1.541 m). However, there were no relevant differences in the respective values corresponding to the various mixtures, with the best value being Lac50_MCC50, as already explained previously. As in arching, the powder mixtures (Lac_MCC) tended towards a plateau with the lowest value corresponding to Lac50_MCC50. The reason for this occurrence was that the friction developed by the MCC particles (smoother, and therefore greater contact with the equipment surface, Figure 2) in relation to the walls of

the funnel was much more evident than that of the Lac particles, which are more irregular and, as already emphasized, have many small particles adhering to the larger ones, which reduces the points of contact with the surfaces. As with arching, internal friction is more evident between Lac than with MCC, with MCC flowing faster in the central area than at the sides, which can cause a channel ratholing form, requiring the use of an outlet with a larger diameter, which ended up being verified. Another analysis that can be made is in relation to size versus shape, highlighting in this case a predominance of the influence of size over shape, apart from what has been described (in this test, the MCC combines smooth surfaces with reduced size, thus providing more surface area contact area) [18,50,51,70]. In the studies already mentioned, the F < 63 of the MCC200 showed a value of 1.132 ± 0.033 m for this parameter, which proved a similar ratholing flow to the MCC value (1.541 ± 0.011 m). The same comparison was also made between FTotal (bulk Lac) and F > 90 (18.84%, *w*/*w*) of LacMN200 used in another study, whose values for this parameter were 0.965 ± 0.010 m and 0.296 ± 0.013 m. The higher value for MCC producing ratholing is easier than Lac and was probably caused by the fact that its particles are smaller (greater surface area), with a more regular surface and no adhering particles, causing more friction with the walls of the equipment. This friction will inhibit the lateral movement of the particles in relation to the central particles, which will cause different speeds in the powder, facilitating the appearance of a rathole (central flow channel) [50]. When the movement of particles is very fast, powder may accumulate at the hopper outlet, causing an increase in σ_1 and, proportionally, in σ_c (more cohesive) in relation to σ_0. When $\sigma_0 < \sigma_c$, the flow of powder is blocked [56,57].

Improvements in flow to prevent both arching and ratholing can be made by increasing the outlet opening or adding glidants [18,56]. The use of CSD in the Lac50_MCC50 showed an improvement in flow with a decrease in the size of the hopper opening. This improvement was more evident in ratholing than in arching, because the effect of the glidant is more pronounced in reducing friction between particle surfaces and equipment surfaces than between interparticle friction forces. In this parameter, the action of the glidant, through its mechanisms already described in this study, reduced the contact of the particles with the walls of the equipment by interposing itself at different points between them, and not by forming a film, leading to a decrease in friction forces with improved flow. The minimum opening value for Lac50_MCC50 was 1.346 + 0.023 m. In arching, this effect is not as pronounced because the interparticle friction forces in Lac50_MCC50 were already reduced, with an outlet opening of 0.144 + 0.007 m [19,56].

When analyzing the two profiles separately, a decrease in the outlet diameter (0.25% = 0.056 ± 0.007 m) was observed for a smaller amount of glidant in the arching (Figure 9). The increase in this excipient causes a new, albeit very slight, reduction in the analyzed parameter (0.50% = 0.038 ± 0.005 m). For higher concentrations, a slight increase in diameter was observed (0.75% = 0.046 ± 0.005 m and 1.00% = 0.040 ± 0.009 m), which does not exceed the value corresponding to that caused by the addition of 0.25%. Given these results, it can be stated that 0.50% CSD was the concentration that caused the greatest reduction in the friction forces between the particles of Lac50_MCC50, which were already low [19,21,22,56]. In ratholing, the initial reduction was more pronounced, showing that 0.25% glidant (0.056 ± 0.007 m), compared to other concentrations, was sufficient to produce the maximum effect, particularly on the friction forces between the particles and the equipment walls (Figure 9). For higher concentrations of this excipient, the effect is reversed, and instead of a decrease in diameter, there is a pronounced increase at 0.50% (0.402 ± 0.004). Subsequent concentrations undergo a slight decrease (0.75% = 0.250 ± 0.010 m and 1.00% = 0.256 ± 0.004 m), but never reach the value produced by the lowest CSD concentration [18,19]. Given these results, it can be stated

that 0.25% glidant produced the maximum effect for this parameter, and that concentrations higher than this produced an interaction between its particles similar to that of the mixture (Lac50_MCC50) under study. Thus, at high concentrations, glidant, instead of creating points between the surfaces of the powder particles and the walls of the equipment to reduce or eliminate the friction forces between them, forms films that behave like a normal powder in relation to the interaction forces between particle surfaces and walls of the equipment.

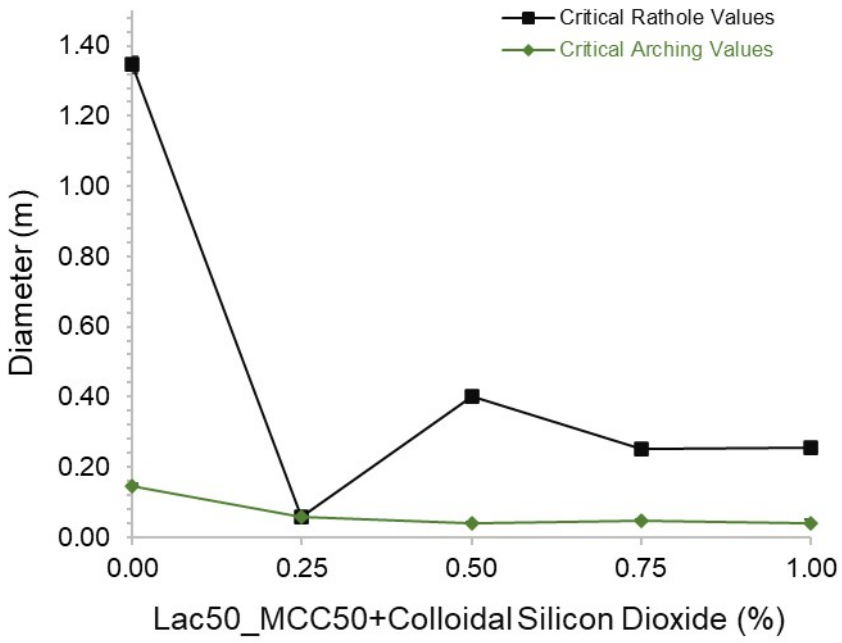


Figure 9. Critical arching and rathole values (in meters) for Lac50:MCC50 and Lac50:MCC50 with glidant discharges.

4. Flow functions

In previous tests, the explanation for powder behavior was primarily based on frictional and mechanical forces between particles, which predominated [47,48,71]. However, in flow functions (FFs), these forces are less relevant than cohesion/adhesion forces. Thus, cohesion can be described as a measure of the binding strength between bound particles [19,47,48].

The results for the flow functions showed that as σ_1 increased, there was a gradual increase in σ_c (Figure 10). This increase resulted from an intensification of interactions between particles (friction, cohesion, and mechanical forces) in the densification process of the "bulk solid." This interaction between particles depends on their surfaces (area, porosity, roughness, van der Waals forces, electrostatic charges, capillarity, and texture) and their proximity to each other. Under the action of σ_1, it allows better or worse compaction of the powder [17,18,50,51,70,72]. Regarding capillary forces, they were not considered in the powders under study because their moisture content does not influence their flow behavior [73,74]. Under the action of σ_1, the improvement in the packing of the powder that led to its densification (bulk solid) resulted from the reduction in voids, with the expulsion of air due to its occupation by smaller particles already existing in the powder or resulting from its fragmentation and/or due to its plastic deformations.

Regarding the profiles obtained in this test (FF) for bulk powders and powder mixtures without glidant, it was possible to observe a similar initial flow behavior among the various powders that started in region $1 < ff_c < 2$, corresponding to very cohesive behavior. These powders had different durations in this region, with the longest being as σ_1 increased to the value corresponding to bulk Lac (7200 Pa), which allowed it to move to region $2 < ff_c < 4$,

corresponding to cohesive behavior, where it remained until the end of the test. The other powders (MCC and powder mixtures without a lubricant) moved to this latter region and, as in the previous case, remained there until the end of the test, at the following σ_1 values: Lac75_MCC25 = 1600 Pa; Lac50_MCC50 = 1000 Pa; Lac25_MCC75 = 700 Pa; and MCC = 900 Pa. The behaviors observed throughout the densification process of the "bulk solid" as the stress parameter σ_1 escalated stemmed from an increased frequency of interactions among particles (predominantly cohesive forces) and the aggregation of finer particles, particularly Lac. These finer particles, alongside those already present, may also emerge from the disintegration of larger particles of this excipient. In the case of MCC, this situation is less likely due to its plastic behavior (ductile), deforming before fragmenting [68,75]. When analyzing all the powders according to the results obtained and considering their spatial profile, shown in Figure 10, the worst was bulk Lac, followed by Lac75_MCC25, with Lac50_MCC50, Lac 25_MCC75, and MCC being practically equal, the latter two mixtures being more efficient at higher σ_1 values. The reason for these behaviors was related to the shape and size of the particles and the proportion of each excipient in each mixture, as already described in the explanation of the other tests of this study. The bulk Lac, despite being larger, presented worse flow, probably due to its irregular shape and immensely smaller particles (Figure 2). Here, the shape factor surpassed the size factor, as observed in another studies [50,70].

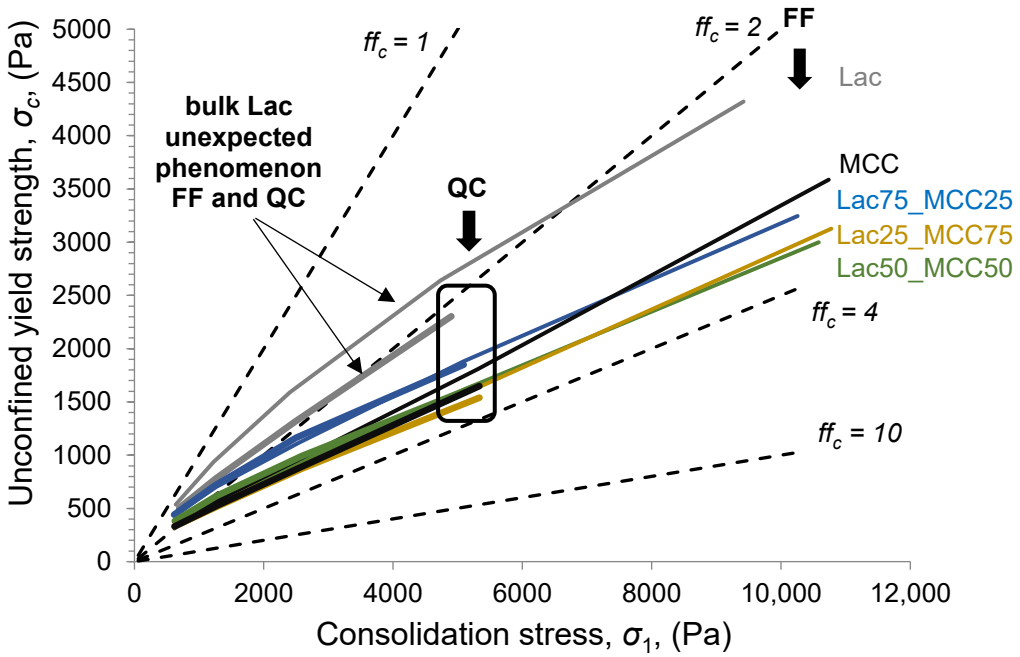


Figure 10. Flow function and QuickTime consolidated flow function of the bulk powder (Lac and MCC) and powder mixtures (Lac_MCC) without glidant.

In relation to all QC profiles, no caking occurred, as there was no increase in the bonding strength (σ_c) of "bulk solid" during storage at rest under a given compressive stress period [18]. However, a phenomenon not expected, which occurred in other works [21,70], was observed with bulk Lac, probably due to the increase in the small particles, resulting from action σ_1 that improved the process of densification of the "bulk solid," leading to the occurrence of the "incipient flow", and failure at lower values of σ_c, which resulted in a less cohesive powder. From this point, the consolidated "bulk solid" starts to flow with increasing ff_c.

Other ff_c values obtained by interpolation with σ_1 varying between 700 and 10,000 Pa allowed for a more concise analysis of the various flows and the different factors that influ-

enced them, more specifically, size and shape, with size not being decisive in determining flow (Figure 11) [17,50,51]). A more detailed analysis showed the overlap of the two profiles, Lac50_MCC50 and Lac25_MCC75, demonstrating similar flow behaviors. Regarding bulk MCC, which was superimposable up to 2000 Pa, from this σ_1 value onwards, it moves away from them to lower ff_c values (worst flow), crossing the Lac75_MCC25 profile near 7800 Pa. Of all the powders, the only one that showed a tendency to form a plateau within the σ_1 range used (0 to 10,000 Pa) was MCC from 5000 Pa, demonstrating that it reached complete consolidation.

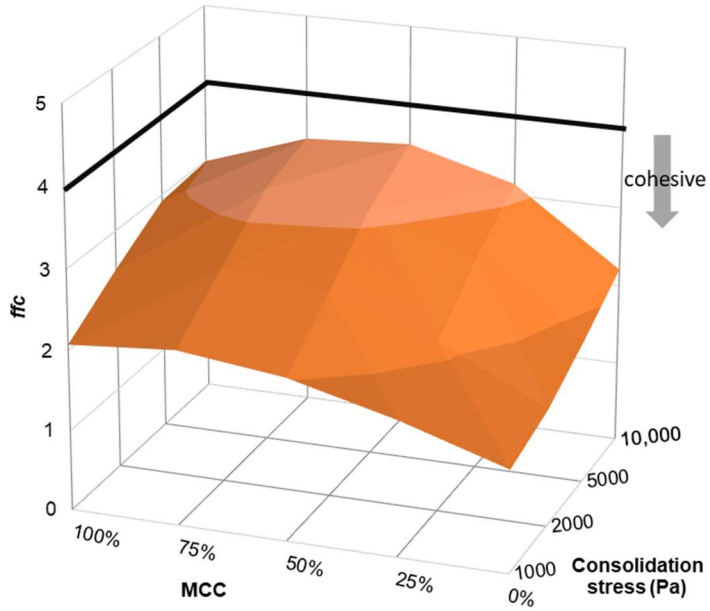


Figure 11. Influence of MCC/Lac ratio and consolidation stress in the flow index, ff_c.

Regarding the profiles of the other phase of this study, which involved the powder mixture (Lac50_MCC50) supplemented with CSD at varying concentrations (Figure 12) and ff_c values obtained by interpolation with σ_1 varying between 700 and 10,000 Pa (Figure 13), it was possible to observe the evident effect of the same on the mixtures' flow behavior. All profiles improve their flow, with Lac50_MCC50+0.25% starting in the region of $2 < ff_c < 4$, corresponding to a cohesive behavior, with a ff_c = 3.6 at σ_1 of 800 Pa; change for the region of $4 < ff_c < 10$, corresponding to easy-flowing at 850 Pa; and remaining in this region until the end of the test, demonstrating that from 4000 Pa, it reached complete consolidation with ff_c = 6.9, giving rise to the occurrence of a plateau. The other profiles corresponding to the remaining powder mixtures with glidant started at ff_c = 5.9, 5.3, and 4.9 (Lac50_MCC50+0.50%, Lac50_MCC50+0.75%, and Lac50_MCC50+1.00%, respectively) at σ_1 of 800 Pa, changing for the free-flowing region ($ff_c > 10$) at σ_1 of 1500 Pa. From there on, there were pronounced increases in ff_c up to 4000 Pa, and then with the consolidation almost complete of "bulk solid", slight increase was verified until the end of the test for Lac50_MCC50+0.75% (the best) and Lac50_MCC50+1.00%. Lac50_MCC+0.50% showed a reduction in ff_c (15.6 to 14.2) between 4000 and 7500 Pa, respectively. Although slight, this reduction requires repetition of this test with a new formulation.

In relation to all QC profiles, no caking occurred of "bulk solids" during storage at rest [18].

All these improvements in Lac50_MCC50 flow behavior with CSD were developed from the action of this glidant, already known, which mainly reduces or nullifies the cohesive/adhesives forces. In other studies [21,22], these values were corroborated, demonstrating that 0.75% is the best percentage for this co-processed excipient, producing a high

increase in ff_c, which is very important for the formulation and production of solid oral dosage forms (SODFs).

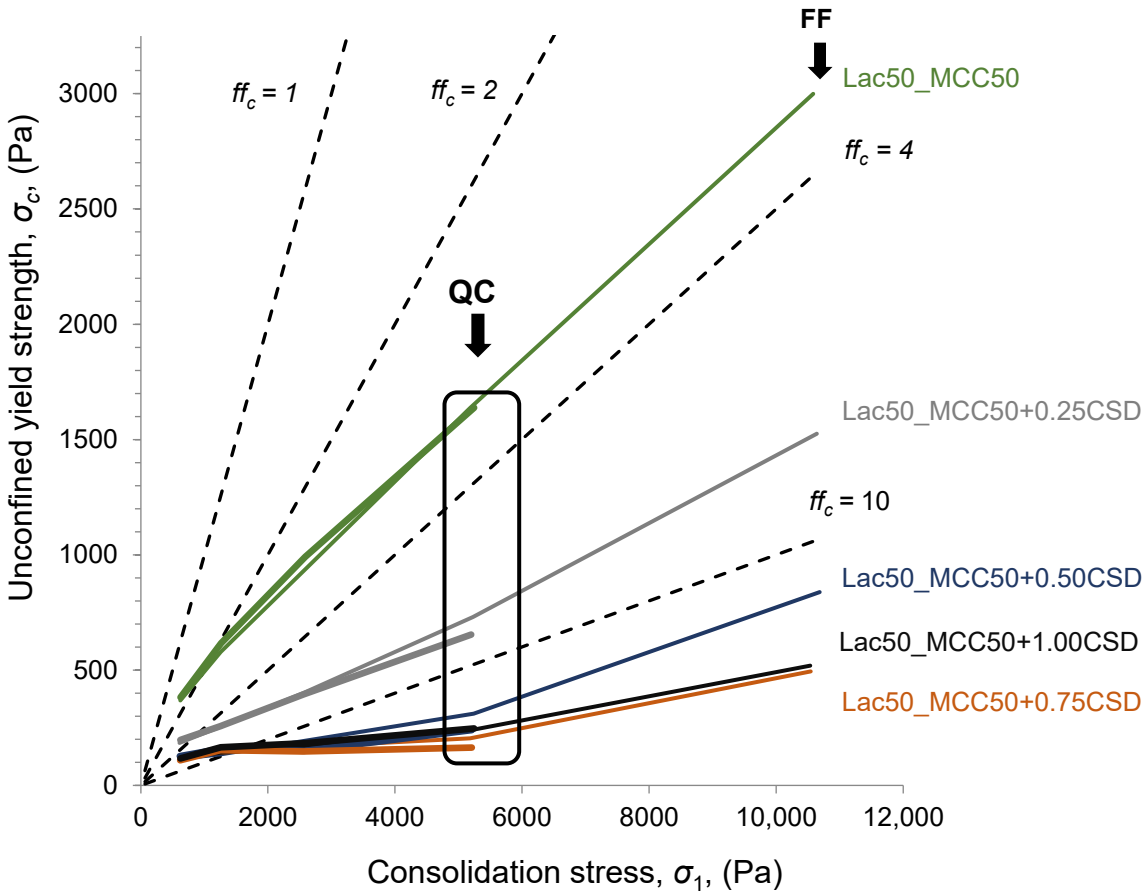


Figure 12. Flow function and QuickTime consolidated flow function of the powder mixture (Lac_MCC) with glidant.

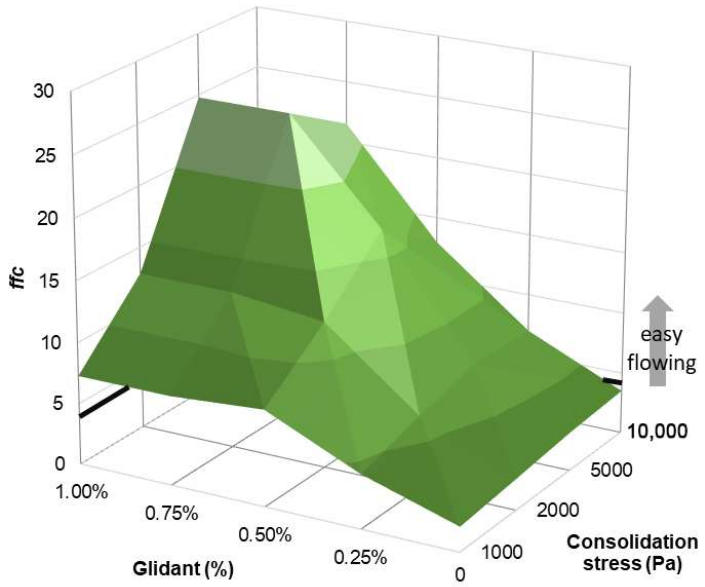


Figure 13. Influence of glidant concentration and consolidation stress in the flow index, ff_c.

4. Conclusions

Powder flowability is a challenge in the formulation and production of solid dosage forms. Many excipients lack good compressibility characteristics, making the process difficult. Based on that, this study analyzed the interaction between Lac and MCC particles, which became known through the characterization of the flow of their mixtures in different proportions using a shear cell. The interparticle forces resulting from each excipient, due to their size and shape, showed that the best ratio, the one that presented the best flow characteristics, was 50:50 (w/w). To further improve the flow behavior of this mixture, the addition of glidant in varying amounts produced a significant improvement in flow behavior, exceeding 10 on the flowability index (ff_c) scale. Furthermore, other results also improved, such as rathole and arching. All these improvements were the result of the action of the CSD, which showed that 0.5% is the minimum concentration to produce the desired effect. With these results, it was concluded that the co-processed product created will be an excellent excipient to produce solid dosage forms in the pharmaceutical industry.

Author Contributions: P.J.S.: Conceptualization, Methodology, Software, Validation, Formal Analysis, Investigation, Writing—Original Draft, Writing—Review and Editing, Visualization, Supervision, Project Administration. D.C.: Methodology, Formal Analysis, Investigation. T.N.: Software, Formal Analysis, Investigation. J.C.: Software, Formal Analysis, Investigation. J.P.S.e.S.: Methodology, Resources, Investigation, Visualization, Supervision, Project Administration. P.J.C.: Conceptualization, Methodology, Software, Validation, Formal Analysis, Investigation, Resources, Data Curation, Writing—Review and Editing, Visualization, Supervision, Project Administration, Funding Acquisition. All authors have read and agreed to the published version of the manuscript.

Funding: This work was financed by national funds from FCT—Fundação para a Ciência e a Tecnologia, I.P., in the scope of the projects UIDP/04378/2020 and UIDB/04378/2020 of the Research Unit on Applied Molecular Biosciences—UCIBIO and the project LA/P/0140/2020 of the Associate Laboratory Institute for Health and Bioeconomy—i4HB.

Institutional Review Board Statement: Not applicable.

Informed Consent Statement: Not applicable.

Data Availability Statement: The original contributions presented in this study are included in the article. Further inquiries can be directed to the corresponding authors.

Conflicts of Interest: José Catita is employed by the company Paralab. The remaining authors declare that this research was conducted in the absence of any commercial or financial relationships that could be construed as potential conflicts of interest.

References

1. Hummler, H.; Stillhart, C.; Meilicke, L.; Grimm, M.; Krause, E.; Mannaa, M.; Gollasch, M.; Weitschies, W.; Page, S. Impact of Tablet Size and Shape on the Swallowability in Older Adults. *Pharmaceutics* **2023**, *15*, 1042. [CrossRef] [PubMed]
2. Garcia-Arieta, A. Interactions between active pharmaceutical ingredients and excipients affecting bioavailability: Impact on bioequivalence. *Eur. J. Pharm. Sci.* **2014**, *65*, 89–97. [CrossRef] [PubMed]
3. Elder, D.P.; Kuentz, M.; Holm, R. Pharmaceutical excipients—Quality, regulatory and biopharmaceutical considerations. *Eur. J. Pharm. Sci.* **2016**, *87*, 88–99. [CrossRef] [PubMed]
4. Pockle, R.D.; Masareddy, R.S.; Patil, A.S.; Patil, P.D. A comprehensive review on pharmaceutical excipients. *Ther. Deliv.* **2023**, *14*, 443–458. [CrossRef]
5. Banker, G.S.; Peck, G.E.; Baley, G. Tablet Formulation and Design. In *Pharmaceutical Dosage Forms: Tablets*; Marcel Dekker: New York, NJ, USA, 1980; pp. 61–109.
6. Burande, A.S.; Dhakare, S.P.; Dondulkar, A.O.; Gatkine, T.M.; Bhagchandani, D.O.; Sonule, M.S.; Thakare, V.M.; Prasad, S.K. A review on the role of co-processed excipients in tablet formulations. *Hybrid Adv.* **2024**, *7*, 100299. [CrossRef]
7. Lachman, L.; Lieberman, H.A.; Kanig, J.L. *The Theory and Practice of Industrial Pharmacy*; Lea & Febiger: Philadelphia, PA, USA, 1976.

8. European Parliament and of the Council. *Directive 2001/83/EC of 6 November 2001 on the Community code Relating to Medicinal Products for Human Use*; Publications Office of the European Union: Luxembourg, 2001.
9. Vasconcelos, T.; Marques, S.; Sarmento, B. The biopharmaceutical classification system of excipients. *Ther. Deliv.* **2017**, *8*, 65–78. [CrossRef]
10. Adewale Adetunji, O. Chemically Modified Starches as Excipients in Pharmaceutical Dosage Forms. In *Chemical Properties of Starch*; Emeje, M., Ed.; IntechOpen: London, UK, 2020.
11. Guth, F.; Schiffter, H.A.; Kolter, K. Novel excipients—From concept to launch. *Chim. Oggi-Chem. Today* **2013**, *31*, 78–81.
12. Kanojia, N.; Kaur, L.; Nagpal, M.; Bala, R. Modified Excipients in Novel Drug Delivery: Need of the Day. *J. Pharm. Technol. Res. Manag.* **2013**, *1*, 81–107. [CrossRef]
13. Kokott, M.; Lura, A.; Breitkreutz, J.; Wiedey, R. Evaluation of two novel co-processed excipients for direct compression of orodispersible tablets and mini-tablets. *Eur. J. Pharm. Biopharm.* **2021**, *168*, 122–130. [CrossRef]
14. Kozarewicz, P.; Loftsson, T. Novel excipients—Regulatory challenges and perspectives—The EU insight. *Eur. J. Pharm.* **2018**, *546*, 176–179. [CrossRef]
15. Bhatia, V.; Dhingra, A.; Chopra, B.; Guarve, K. Co-processed excipients: Recent advances and future perspective. *J. Drug Deliv. Sci. Technol.* **2022**, *71*, 103316. [CrossRef]
16. Pingali, K.; Mendez, R.; Lewis, D.; Michniak-Kohn, B.; Cuitino, A.; Muzzio, F. Mixing order of glidant and lubricant—Influence on powder and tablet properties. *Int. J. Pharm.* **2011**, *409*, 269–277. [CrossRef] [PubMed]
17. Salústio, P.J.; Inacio, C.; Nunes, T.; Silva, J.P.S.E. Flow characterization of a pharmaceutical excipient using the shear cell method. *Pharm. Dev. Technol.* **2020**, *25*, 237–244. [CrossRef] [PubMed]
18. Schulze, D. Flow properties of bulk solids. In *Powders Bulk Solids: Behavior Characterization Storage Flow*; Schulze, D., Ed.; Springer: Berlin/Heidelberg, Germany; New York, NY, USA; Tokyo, Japan, 2008; pp. 35–74.
19. Jager, P.D.; Bramante, T.; Luner, P.E. Assessment of Pharmaceutical Powder Flowability using Shear Cell-Based Methods and Application of Jenike's Methodology. *J. Pharm. Sci.* **2015**, *104*, 3804–3813. [CrossRef]
20. Jonat, S.; Hasenzahl, S.; Gray, A.; Schmidt, P.C. Mechanism of glidants: Investigation of the effect of different colloidal silicon dioxide types on powder flow by atomic force and scanning electron microscopy. *J. Pharm. Sci.* **2004**, *93*, 2635–2644. [CrossRef]
21. Salústio, P.J.; Machado, M.; Nunes, T.; Silva, J.P.S.E.; Costa, P.C. Influence of the Glidant on Diluent Flow Characterization Using Shear Cell Method. *J. Pharm. Innov.* **2020**, *17*, 60–70. [CrossRef]
22. Salustio, P.J.; Monteiro, M.F.; Nunes, T.; Silva, J.P.S.E.; Costa, P.J. Starch flow behavior alone and under different glidants action using the shear cell method. *Drug Dev. Ind. Pharm.* **2021**, *47*, 1502–1511. [CrossRef]
23. Chowhan, Z.T.; Yang, I.C. Powder flow studies IV. Tensile strength and orifice flow rate relationships of binary mixtures. *Int. J. Pharm.* **1983**, *14*, 231–242. [CrossRef]
24. Li, J.; Wu, Y. Lubricants in Pharmaceutical Solid Dosage Forms. *Lubricants* **2014**, *2*, 21. [CrossRef]
25. Tadauchi, T.; Yamada, D.; Koide, Y.; Yamada, M.; Shimada, Y.; Yamazoe, E.; Ito, T.; Tahara, K. Improving the Powder Properties of an Active Pharmaceutical Ingredient (Ethenzamide) with a Silica Nanoparticle Coating for Direct Compaction into Tablets. *Powders* **2022**, *1*, 231–242. [CrossRef]
26. Jones, T.M.; Pilpel, N. The flow of granular magnesia. *J. Pharm. Pharmacol.* **1966**, *18*, 429–442. [CrossRef] [PubMed]
27. Gold, G.; Duvall, R.N.; Palermo, B.T.; Slater, J.G. Powder flow studies 3. Factors affecting the flow of lactose granules. *J. Pharm. Sci.* **1968**, *57*, 667–671. [CrossRef] [PubMed]
28. Meyer, K.; Zimmermann, I. Effect of glidants in binary powder mixtures. *Powder Technol.* **2004**, *139*, 40–54. [CrossRef]
29. Sunkara, D.; Capece, M. Influence of Material Properties on the Effectiveness of Glidants Used to Improve the Flowability of Cohesive Pharmaceutical Powders. *AAPS PharmSciTech* **2018**, *19*, 1920–1930. [CrossRef]
30. Blanco, D.; Antikainen, O.; Raikkonen, H.; Yliruusi, J.; Juppo, A.M. Effect of colloidal silicon dioxide and moisture on powder flow properties: Predicting in-process performance using image-based analysis. *Int. J. Pharm.* **2021**, *597*, 120344. [CrossRef]
31. Chen, Y.H.; Yang, J.; Dave, R.N.; Pfeffer, R. Fluidization of coated group C powders. *Aiche J.* **2008**, *54*, 104–121. [CrossRef]
32. Kumar, R.; Wagoner, S.; Cummings, J.; Tsolaki, E.; Oliveira, M.A.; Worku, Z.A.; Chiarella, R.A. Influence of colloidal silicon dioxide-magnesium stearate interaction on flow and compaction behavior of an MCC-Lactose binary mixture. *Powder Technol.* **2024**, *434*, 119371. [CrossRef]
33. Otles, S.; Lecoq, O.; Dodds, J.A. Dry particle high coating of biopowders: An energy approach. *Powder Technol.* **2011**, *208*, 378–382. [CrossRef]
34. Jonat, S.; Albers, P.; Gray, A.; Schmidt, P.C. Investigation of the glidant properties of compacted colloidal silicon dioxide by angle of repose and X-ray photoelectron spectroscopy. *Eur. J. Pharm. Biopharm.* **2006**, *63*, 356–359. [CrossRef]
35. Garavito, M.C.J.; Pacheco, M.G.C.; Gerardin, F.; Falk, V. Silica Nanoparticles as Glidants for Industrial Processing: A Statistical Approach. *Ind. Eng. Chem. Res.* **2022**, *61*, 16517–16528. [CrossRef]
36. European Commission. *Commission Recommendation of 10 June 2022 on the Definition of Nanomaterial*; 2022/C 229/01; European Commission: Brussels, Belgium, 2022.

37. EDQM Council of Europe (Ed.) Powder Flow Properties by Shear Cell Methods. In *European Pharmacopoeia*, 11th ed.; Chapter 2.9.49; EDQM Council of Europe: Strasbourg, France, 2023.
38. EDQM Council of Europe (Ed.) Flowability. In *European Pharmacopoeia*, 11th ed.; Chapter 2.9.16; EDQM Council of Europe: Strasbourg, France, 2023.
39. EDQM Council of Europe (Ed.) Bulk Density and Tapped Density of Powders. In *European Pharmacopoeia*, 11th ed.; Chapter 2.9.34; EDQM Council of Europe: Strasbourg, France, 2023.
40. EDQM Council of Europe (Ed.) Powder Flow. In *European Pharmacopoeia*, 11th ed.; Chapter 2.9.36; EDQM Council of Europe: Strasbourg, France, 2023.
41. Rios, M. Developments in Powder Flow Testing. *Pharm. Technol.* **2006**, *30*, 38–49.
42. Abdullah, E.C.; Geldart, D. The use of bulk density measurements as flowability indicators. *Powder Technol.* **1999**, *102*, 151–165. [CrossRef]
43. Tharanon, W.; Guo, Y.; Peerapattana, J.; Sun, C.C. A systematic comparison of four pharmacopoeial methods for measuring powder flowability. *Int. J. Pharm.* **2024**, *661*, 124454. [CrossRef] [PubMed]
44. Leturia, M.; Benali, M.; Lagarde, S.; Ronga, I.; Saleh, K. Characterization of flow properties of cohesive powders: A comparative study of traditional and new testing methods. *Powder Technol.* **2014**, *253*, 406–423. [CrossRef]
45. Carr, R. Evaluating flow properties of solids. *Chem. Eng.* **1965**, *72*, 163–168.
46. Gaikwad, S.S.; Kothule, A.M.; Morade, Y.Y.; Patil, S.S.; Laddha, U.D.; Kshirsagar, S.J.; Salunkhe, K.S. An overview of the implementation of SeDeM and SSCD in various formulation developments. *Int. J. Pharm.* **2023**, *635*, 122699. [CrossRef]
47. Wang, Y.F.; Koynov, S.; Glasser, B.J.; Muzzio, F.J. A method to analyze shear cell data of powders measured under different initial consolidation stresses. *Powder Technol.* **2016**, *294*, 105–112. [CrossRef]
48. Leung, L.Y.; Mao, C.; Srivastava, I.; Du, P.; Yang, C.Y. Flow Function of Pharmaceutical Powders Is Predominantly Governed by Cohesion, Not by Friction Coefficients. *J. Pharm. Sci.* **2017**, *106*, 1865–1873. [CrossRef]
49. Salústio, P.J.; Amaral, M.H.; Costa, P.C. Different Carriers for Use in Dry Powder Inhalers: Characteristics of Their Particles. *J. Aerosol Med. Pulm. Drug Deliv.* **2024**, *37*, 307–327. [CrossRef]
50. Salústio, P.J.; Pais, B.V.; Malta, T.; Nunes, T.; Silva, J.P.S.E.; Costa, P.J. Flow behavior under shear cell analysis of two HMPC grades. *Powder Technol.* **2023**, *430*, 119025. [CrossRef]
51. Salústio, P.J.; Machado, M.; Nunes, T.; Silva, J.P.S.E.; Costa, P.C. Lactose monohydrate flow characterization using shear cell method. *Pharm. Dev. Technol.* **2020**, *25*, 686–693. [CrossRef] [PubMed]
52. Ketterhagen, W.R.; Curtis, J.S.; Wassgren, C.R.; Hancock, B.C. Predicting the flow mode from hoppers using the discrete element method. *Powder Technol.* **2009**, *195*, 1–10. [CrossRef]
53. Hancock, B.C. The Wall Friction Properties of Pharmaceutical Powders, Blends, and Granulations. *J. Pharm. Sci.* **2019**, *108*, 457–463. [CrossRef] [PubMed]
54. USP <1063> Shear Cell Methodology for Powder Flow Testing in United States Pharmacopeia National, Formulary, U.S.P. Convention, Rockville, MD, USA, 2025. Available online: https://www.researchgate.net/publication/286054447_Proposed_new_USP_general_information_chapter_Shear_cell_methodology_for_powder_flow_testing_1063 (accessed on 30 October 2025).
55. Hill, J.M.; Cox, G.M. Rat-hole stress profiles for shear-index granular materials. *Acta Mech.* **2002**, *155*, 157–172. [CrossRef]
56. Leung, L.Y.; Mao, C.; Pieters, S.R.; Yang, C.Y. A Proposed Complete Methodology to Predict Gravity Flow Obstruction of Pharmaceutical Powders in Drug Product Manufacturing. *J. Pharm. Sci.* **2019**, *108*, 464–475. [CrossRef]
57. Jenike, A.W. *Gravity Flow of Bulk Solids*; University of Utah: Salt Lake City, UT, USA, 1961.
58. Zhao, H.; Zhao, L.; Lin, X.; Shen, L. An update on microcrystalline cellulose in direct compression: Functionality, critical material attributes, and co-processed excipients. *Carbohydr. Polym.* **2022**, *278*, 118968. [CrossRef]
59. Lin, Z.; Cabello, B.; Dave, R.N. Impact of dry coating lactose as a brittle excipient on multi-component blend processability. *Int. J. Pharm.* **2024**, *653*, 123921. [CrossRef]
60. EDQM Council of Europe (Ed.) Particle-Size Distribution Estimation by Analytical Sieving. In *European Pharmacopoeia*, 11th ed.; Chapter 2.9.38; EDQM Council of Europe: Strasbourg, France, 2023.
61. EDQM Council of Europe (Ed.) Particle Size Analysis by Laser Light Diffraction. In *European Pharmacopoeia*, 11th ed.; Chapter 2.9.31; EDQM Council of Europe: Strasbourg, France, 2023.
62. Amidon, G.E.; Houghton, M.E. The effect of moisture on the mechanical and powder flow properties of microcrystalline cellulose. *Pharm. Res.* **1995**, *12*, 923–929. [CrossRef]
63. Modugno, C.; Paterson, A.J.H.; McLeod, J. Lactose caking: Influence of the particle size distribution and the water content. *Procedia Eng.* **2015**, *102*, 114–122. [CrossRef]
64. Lu, X.Y.; Chen, L.; Wu, C.Y.; Chan, H.K.; Freeman, T. The Effects of Relative Humidity on the Flowability and Dispersion Performance of Lactose Mixtures. *Materials* **2017**, *10*, 592. [CrossRef]
65. Sun, C.C. Quantifying effects of moisture content on flow properties of microcrystalline cellulose using a ring shear tester. *Powder Technol.* **2016**, *289*, 104–108. [CrossRef]

66. Al-Hashemi, H.M.B.; Al-Amoudi, O.S.B.A. review on the angle of repose of granular materials. *Powder Technol.* **2018**, *330*, 397–417. [CrossRef]
67. Rackl, M.; Grotsch, F.E.; Rusch, M.; Fottner, J. Qualitative and quantitative assessment of 3D-scanned bulk solid heap data. *Powder Technol.* **2017**, *321*, 105–118. [CrossRef]
68. Hou, H.; Sun, C.C. Quantifying effects of particulate properties on powder flow properties using a ring shear tester. *J. Pharm. Sci.* **2008**, *97*, 4030–4039. [CrossRef]
69. Seppala, K.; Heinamaki, J.; Hatara, J.; Seppala, L.; Yliruusi, J. Development of a new method to get a reliable powder flow characteristics using only 1 to 2 g of powder. *AAPS PharmSciTech* **2010**, *11*, 402–408. [CrossRef]
70. Salústio, P.J.; Silva, L.; Nunes, T.; Silva, J.P.S.E.; Costa, P.J. Mannitol flowability size/stress threshold limit. *Powder Technol.* **2025**, *464*, 121263. [CrossRef]
71. Brubaker, J.; Moghtadernejad, S. A Comprehensive Review of the Rheological Properties of Powders in Pharmaceuticals. *Powders* **2024**, *3*, 233–254. [CrossRef]
72. Zafar, U.; Vivacqua, V.; Calvert, G.; Ghadiri, M.; Cleaver, J.A.S. A review of bulk powder caking. *Powder Technol.* **2017**, *313*, 389–401. [CrossRef]
73. Faqih, A.M.; Mehrotra, A.; Hammond, S.V.; Muzzio, F.J. Effect of moisture and magnesium stearate concentration on flow properties of cohesive granular materials. *Int. J. Pharm.* **2007**, *336*, 338–345. [CrossRef]
74. Crouter, A.; Briens, L. The effect of moisture on the flowability of pharmaceutical excipients. *AAPS PharmSciTech* **2014**, *15*, 65–74. [CrossRef]
75. Janssen, P.H.M.; Jaspers, M.; Meier, R.; Roelofs, T.P.; Dickhoff, B.H.J. The effect of excipient particle size on the reduction of compactibility after roller compaction. *Int. J. Pharm. X* **2022**, *4*, 100117. [CrossRef]

Disclaimer/Publisher's Note: The statements, opinions and data contained in all publications are solely those of the individual author(s) and contributor(s) and not of MDPI and/or the editor(s). MDPI and/or the editor(s) disclaim responsibility for any injury to people or property resulting from any ideas, methods, instructions or products referred to in the content.